Supplementary Materials

Peroxymonosulfate activation by Fe/C composites for paracetamol degradation: Performance evaluation and mechanism insight

Number of pages: 25

Number of texts: 8

Number of tables: 8

Number of Figures: 16

Texts

Text S1. Chemicals.

The chemicals were purchased from Shanghai Aladdin Chemistry Inc., China., and all of the reagents were used without further purification. 1,10-phenanthroline monohydrate ($C_{12}H_8N_2 \cdot H_2O$, 98%), iron sulfate heptahydrate ($FeSO_4 \cdot 7H_2O$, 99%), ethanol (EtOH, C_2H_6O, 99.5%), hydrochloric acid (HCl, ≥ 98%), peroxymonosulfate (PMS, 42%~46% $KHSO_5$ basis), paracetamol (PCT, $C_8H_9NO_2$, 98%), sodium thiosulfate pentahydrate ($Na_2S_2O_3 \cdot 5H_2O$, > 99.0%), sodium chloride (NaCl, 99.5%), sodium nitrate ($NaNO_3$, 99%), sodium sulfate (Na_2SO_4, 99%), sodium carbonate (Na_2CO_3, 99.5%), sodium hydrogen carbonate ($NaHCO_3$, 99%), sodium perchlorate monohydrate ($NaClO_4 \cdot H_2O$, 98%), humic acid (HA, ≥ 90.0%), p-chloroaniline (PCA, C_6H_6ClN, > 99.5%), rhodamine B (RhB, $C_{28}H_{31}ClN_2O_3$, ≥ 98%), benzoic acid (BA, $C_7H_6O_2$, 99.5%), sulfamethazine (SMZ, $C_{12}H_{14}N_4O_2S$, ≥ 99%), naproxen (NPX, $C_{14}H_{14}O_3$, ≥ 99%), methanol (MeOH, CH_4O, 99.9%), tert-butyl alcohol (TBA, $C_4H_{10}O$, 98.5%), p-benzoquinone (p-BQ, $C_6H_4O_2$, 98%), furfuryl alcohol (FFA, $C_5H_{10}O_2$, 98%), nitrotetrazolium blue chloride (NBT, $C_{40}H_{30}N_{10}O_6 \cdot 2Cl$, NBT, ≥ 98%), β-carotene ($C_{40}H_{56}$, ≥ 96%), deuterium oxide (D_2O, > 99%), dimethyl sulfoxide (DMSO, C_2H_6SO, 99.5%), 5,5-dimethyl-1-pyrroline N-oxide (DMPO, 97%), 2,2,6,6-tetramethyl-4-piperidone (TEMP, 99%), potassium dichromate ($K_2Cr_2O_7$, 99%),

potassium thiocyanate (KSCN, ≥ 98.5%).

Text S2. Characterizing methods.

The morphology and microfeatures of the catalyst were examined using scanning electron microscopy (SEM, TESCAN MIRA LMS, Tescan, Brno, Czech Republic). The crystalline structure of the catalyst was characterized by X-ray diffraction (XRD, Rigaku SmartLab SE, Rigaku Corporation, Akishima, Japan). X-ray photoelectron spectroscopy (XPS, Thermo Scientific K-Alpha, Thermo Fisher Scientific, Waltham, MA, USA) was used to analyze the surface elements and chemical composition of the catalyst. The Brunauer-Emmett-Teller (BET) specific surface area and pore size distribution of the catalysts were determined by N_2 adsorption-desorption test method using an automatic specific surface area analyzer (Micromeritics ASAP 2460, Micromeritics, Atlanta, GA, USA). The Fe content in the catalyst was determined using inductively coupled plasma optical emission spectroscopy (ICP-OES, Agilent 5800, Santa Clara, CA, USA). The electrochemical impedance spectroscopy (EIS) of the catalyst was measured using an electrochemical workstation (CHI760E, Shanghai Chenhua Instrument Co., Ltd., Shanghai, China). The changes in surface functional groups of the sample were analyzed using Fourier transform infrared spectrometer (FT-IR, Thermo Scientific Nicolet Is20, Thermo

Fisher Scientific, Waltham, MA, USA).

Text S3. The determination of Fe content in activators by ICP-OES.

Pre-treatment of ICP-OES: The catalyst (30 mg) was transferred to a 50 mL uncovered porcelain crucible, heated to 800°C at a rate of 10°C/min in a muffle furnace, and held at 800°C for 30 minutes. After cooling to room temperature, 5 mL of concentrated nitric acid was added to the porcelain crucible to completely dissolve the obtained powder, and the solution was then diluted to 100 mL with distilled water.

ICP-OES test was measured by Agilent 7700, and the concentration after digestion was analyzed using the following formula.

$$C_x\left(\frac{mg}{kg}\right) = \frac{C_0\left(\frac{mg}{L}\right) * f * V_0(mL) * 10^{-3}}{m_0(g) * 10^{-3}} = \frac{C_1\left(\frac{mg}{L}\right) * V_0(mL) * 10^{-3}}{m_0(g) * 10^{-3}} \quad \text{(S1)}$$

$$W(\%) = \frac{C_x\left(\frac{mg}{kg}\right)}{10^6} * 100\% \quad \text{(S2)}$$

$$C_1\left(\frac{mg}{L}\right) = C_0\left(\frac{mg}{L}\right) * f \quad \text{(S3)}$$

m_0: when analyzing the sample, the quality of the sample, in grams (g), is recorded by the analytical balance.

V_0: After the sample is digested, the volume of constant volume is in milliliters (mL).

C_0: Test the concentration of elements in the solution, in milligrams per

liter (mg/L). (This data is obtained from the instrument test.)

C_1: The elemental concentration of the original solution of the sample digestion solution, in milligrams per liter (mg/L), calculated using formula (S3). If the sample is a liquid that can be directly tested, C_1 is the final test result.

C_x: The final test result of the measuring element calculated by formula (S1) above, in milligrams per kilogram (mg/kg).

W(%): The final test result of the measurement element expressed as a percentage calculated by formula (S2).

Text S4. The experimental method of electrochemical impedance spectroscopy (EIS).

The electrochemical impedance spectroscopy (EIS) measurements of the activator were performed in a three-electrode system with a 50 mM Na_2SO_4 solution as the electrolyte. The reference, counter, and working electrode used were Ag/AgCl electrode, platinum electrode, and carbon electrode loaded with the catalyst, respectively. To prepare the catalyst-loaded carbon electrode, 3.0 mg of Fe-N-C_x powder was ultrasonically dispersed for 0.5 hours in a mixture consisting of 100 μL of Nafion solution (5 wt%, DuPont), 500 μL of isopropanol, and 500 μL of deionized water. A total of 80 μL of the resulting ink was then pipetted onto a 2 × 2 × 2 cm piece of

carbon electrode, which was subsequently dried at room temperature for 12 hours. This process was repeated once for this side and twice for the other side of the carbon electrode to ensure an even coating of the catalyst. Prior to EIS measurements, the open-circuit potential (OCP) of the system was measured, as this is a key parameter for setting up the EIS measurement. EIS was performed over a frequency range of 1 Hz to 1000000 Hz with an amplitude of 5 mV. The EIS measurements were performed using an electrochemical workstation (CHI760e, Shanghai Chenhua).

Text S5. Measurement of PMS concentration by the ABTS colorimetric method.

The PMS concentration in the system was determined using UV spectrophotometry, with 2,2′-azino-bis (3-ethylbenzothiazoline-6-sulfonic acid) diammonium salt (ABTS) as the chromogenic agent. An aliquot of 0.2 mL of the sample was filtered through a 0.45 μm glass fiber syringe filter. Then, 10 mL of Milli-Q water, 0.4 mL of ABTS (10 mM), and 0.2 mL of Co^{2+} (10 mM) were immediately added to the sample and allowed to react for 10 minutes, forming a green-colored ABTS radical cation. The resulting solution was analyzed using a UV-vis spectrophotometer (UV-2550) at the maximum absorbance wavelength (λ_{max}) of 735 nm.

Text S6. Electrochemical measurements.

All electrochemical analyses were conducted in a three-electrode system comprising an Ag/AgCl electrode as the reference electrode, a platinum electrode as the auxiliary electrode, and a carbon electrode loaded with the activator as the working electrode. Measurements were carried out using an electrochemical workstation (CHI760e, Shanghai Chenhua) with a 50 mM Na_2SO_4 solution as the electrolyte. Details of the preparation of the carbon electrode loaded with the activator are provided in Text S3.

Open Circuit Potential-Time: After the open-circuit potential (OCP) of the system stabilized, PMS and PCT were introduced sequentially at specific time points and measured using the electrochemical workstation.

Amperometric i-t curve (it)： The it experiment was conducted similarly to the OCPT experiment, but with the initial voltage set to the open-circuit potential of the system, and all other procedures remained the same.

Cyclic Voltammetry (CV)： The cyclic voltammetry measurement was conducted between -0.2 ~ 0.8 V vs. Ag/AgCl at a scan rate of 50 mV/s.

Text S7. The experimental method of galvanic oxidation processes (GOP).

The galvanic oxidation process (GOP), introduced by Huang et al., is a technique designed to detect the catalyst-mediated electron transfer occurring in the system[1]. The specific experimental procedure is as follows: two carbon paper electrodes loaded with the activator were placed in two separate half-cells, each containing either the pollutants or PMS. The two half-cells were connected using a U-shaped glass tube filled with agar salt bridge to maintain electrical neutrality during the reaction. The two carbon paper electrodes were connected via wires in an external circuit to form a closed loop, and an ammeter was used to monitor changes in the current flowing through the external circuit. Details on the preparation of the carbon electrodes loaded with the activator are provided in Text S3.

Text S8. Analytical method of LC-MS.

The degradation intermediates of PCT were analyzed using an Agilent 1290 ultrahigh performance liquid chromatography-mass spectrometry (HPLC-MS) system (Bruker maXis impact) with a Zorbax Rx-C18 column. The mobile phase consisted of LC-MS grade ultra-pure water

(A) and methanol (B) at a flow rate of 0.2 mL/min. The elution program started with 90% methanol for 10 minutes, followed by 10% methanol for 3 minutes, then rapidly returned to 90% methanol within 0.1 minutes, holding for an additional 2.9 minutes. The mass spectrometer operated in positive ion mode, scanning an m/z range of 40–500.

Tables

Table S1. HPLC analysis parameters for different pollutants.

pollutant	mobile phase	ratio	flow rate (mL/min)	detection wavelength (nm)
paracetamol (PCT)	methanol/water	40/60	1.0	248
sulfamethazine (SMZ)	methanol/water	55/45	0.8	266
naproxen (NPX)	Methanol/water (pH=2.5)	75/25	1.0	230
p-chloroaniline (PCA)	methanol/water	70/30	1.0	244
benzoic acid (BA)	Methanol/water (pH=3.0)	60/40	1.0	227

Table S2. BET surface area、pore volume and pore size of Fe-N-C_x.

	BET surface area (m^2/g)	Pore volume (cm^3/g)	Pore size (nm)
Fe-N-$C_{0.25}$	66.7685	0.226100	13.5453
Fe-N-$C_{0.75}$	46.3036	0.181018	15.6374
Fe-N-$C_{1.5}$	14.5021	0.093129	20.6346
Fe-N-C_3	13.0664	0.090876	27.8196
Fe-N-C_6	0.4713	0.001417	12.0241

Table S3. ICP-OES test of different catalysts.

	m_0 (mg)	V_0 (mL)	C_0 (mg/L)	f	C_1 (mg/L)	C_x (mg/kg)	Fe content (wt. %)
Fe-C-$N_{0.25}$	30.0	100	6.1971	10	61.9710	206568.8889	20.6569
Fe-C-$N_{0.75}$	31.6	100	6.0514	10	60.5140	191500.0000	19.1500
Fe-C-$N_{1.5}$	31.1	100	5.5098	10	55.0980	177163.9871	17.7164
Fe-C-N_3	30.6	100	4.1893	10	41.8930	136906.3181	13.6906
Fe-C-N_6	31.2	100	2.2895	10	22.8950	73382.4786	7.3382

Table S4. The surface element chemical states of different catalysts. (XPS analysis)

		Fe-N-$C_{0.25}$	Fe-N-$C_{0.75}$	Fe-N-$C_{1.5}$	Fe-N-C_3	Fe-N-C_6
C 1s	C-C	67.51%	65%	65.63%	72.53%	83.12%
	C-O	18.4%	19.54%	17.84%	15.76%	9.03%
	C=O	11.41%	12.14%	13.22%	10.47%	7.85%
	Π-Π	2.68%	3.32%	3.31%	1.25%	0%
N 1s	Pyridinic N	27.14%	24.76%	26.59%	32.58%	43.84%
	Fe-N_X	24.57%	28.92%	28.72%	19.71%	17.5%
	Pyrrolic N	26.45%	26.51%	24.87%	32.81%	17.67%
	Graphitic N	14.12%	13.31%	14.54%	8.01%	5.68%
	N-oxides	7.72%	6.51%	5.28%	6.83%	15.32%
O 1s	C=O	59.1%	73.31%	62.24%	60.44%	67.47%
	C-O-C/C-OH	40.9%	26.69%	37.76%	39.56%	32.53%
Fe 2p	Fe^{2+}	33.24%	34.64%	40.16%	39.42%	66.7%
	Fe^{3+}	66.76%	65.36%	59.84%	60.58%	33.3%

Table S5. Comparison of reported iron-based catalysts.

Catalysts	Pollutant (mg/L)	Activator dosage (mM)	Time (min)	Removal efficiency (%)	Fe-leaching (mg/L)	Refs.
Fe_3C (0.1 g/L)	BPA 0.01 mM	PMS 1.0 mM	10	100	0.13	[2]
GM88 (0.75 g/L)	LVX 30 mg/L	PMS 2.5 mM	150	86	1.1	[3]
Fe(BDC)(DMF,F)-OA-30 (10.0 g/L)	TBBPA 0.018 mM	PMS 3.6 mM	120	90.13	1.51	[4]
Fe@NCNT-BC-800 (1.0 g/L)	RhB 20 mg/L	PDS 5.0 mM	15	100	0.18	[5]
Fe–Co@N-BC (0.2 g/L)	MO 13 mg/L	PDS 4.0 mM	60	85.1	0.239	[6]
Fe-N-C 900 (0.1 g/L)	PCT 10 mg/L	PMS 1.0 mM	30	100	\	[7]
4Fe-N-C (0.03 g/L)	PCT 10 mg/L	PMS 3.0 mM	5	100	\	[8]
Fe/Co_2-MOF (0.05 g/L)	PCT 10 mg/L	PMS 0.8 mM	15	100	\	[9]
Fe@NC-1 (0.05 g/L)	PCT 10 mg/L	PMS 1.0 mM	8	100	\	[10]
Fe-N@C (0.1 g/L)	PCT 10 mg/L	PMS 0.5 mM	30	100	\	[11]
Fe-N-$C_{1.5}$ (0.02 g/L)	PCT 10 mg/L	PMS 1.0 mM	7	100	0.084	This work

Table S6. Comparison of the solution pH before and after adding PMS.

Before adding PMS	pH=3	pH=5	pH=7	pH=9	pH=11
After adding PMS	pH =2.94	pH =3.35	pH =3.36	pH =3.39	pH =10.12

Table S7. Comparison of the surface element chemical states before and after reaction of Fe-N-$C_{1.5}$. (XPS analysis)

		Fe-N-$C_{1.5}$ (Before reaction)	Fe-N-$C_{1.5}$ (After reaction)
C1s	C-C	65.63%	62.27%
	C-O	17.84%	23.52%
	C=O	13.22%	11.18%
	Π-Π	3.31%	3.03%
N1s	Pyridinic N	26.59%	25.85%
	Fe-N_X	28.72%	26.15%
	Pyrrolic N	24.87%	30.42%
	Graphitic N	14.54%	12.67%
	N-oxides	5.28%	4.92%
O1s	C=O	62.24%	50.68%
	C-O-C/C-OH	37.76%	49.32%
Fe2p	Fe^{2+}	40.16%	32.67%
	Fe^{3+}	59.84%	67.33%

Table S8. The intermediate products of PCT degradation.

Products	Molecular formula	Mass (m/z)
PCT	$C_8H_9NO_2$	151
A	$C_{16}H_{16}N_2O_4$	300
B	$C_{16}H_{16}N_2O_4$	300
C	$C_8H_7NO_2$	149
D	$C_8H_7NO_4$	181

E	$C_4H_{11}NO_3$	121
F	C_3H_9NO	75
G	C_2H_5NO	59

Figures

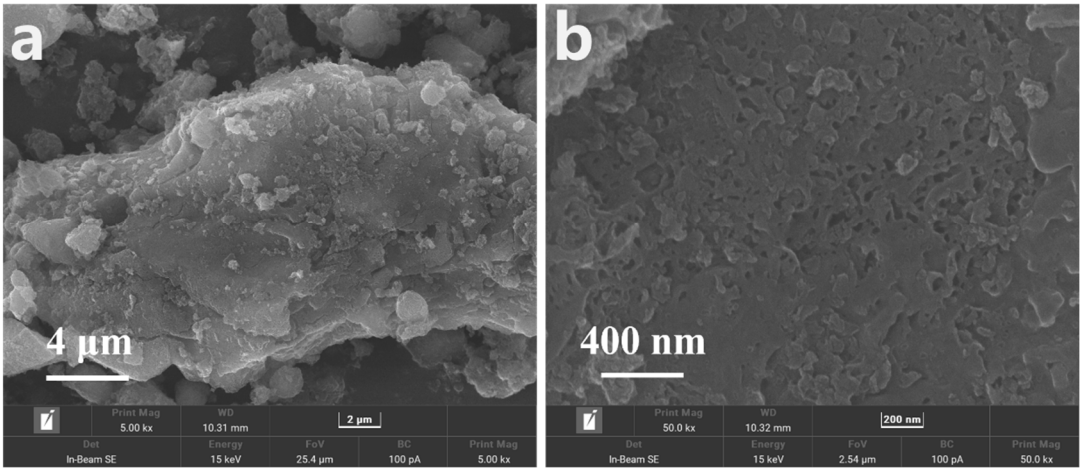


Figure S1. (a, b) SEM images of Fe-N-$C_{0.25}$

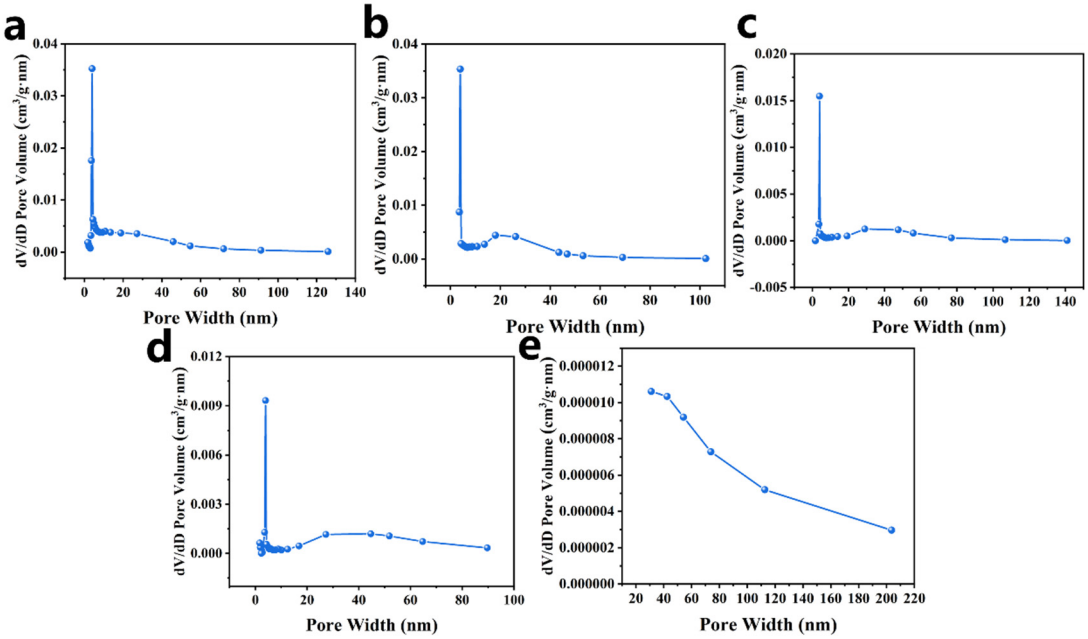


Figure S2. Pore size distribution of Fe-N-$C_{0.25}$ (a), Fe-N-$C_{0.75}$ (b), Fe-N-$C_{1.5}$ (c), Fe-N-C_3 (d) and Fe-N-C_6 (e).

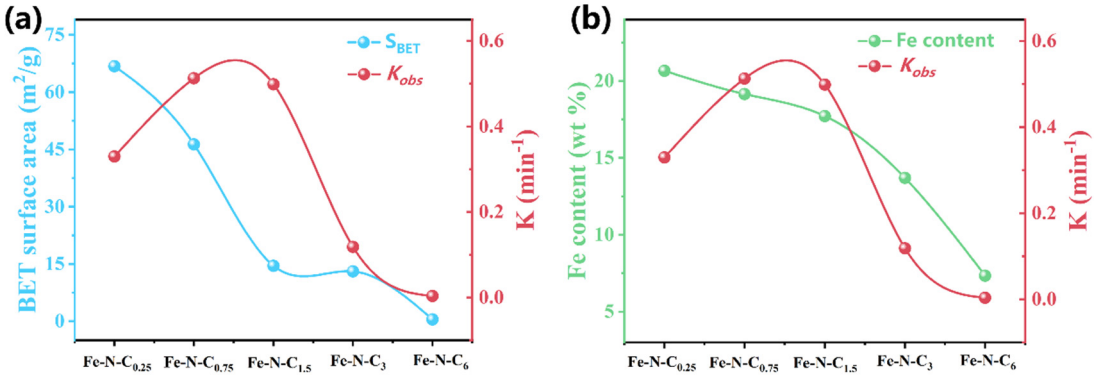


Figure S3. Structure-property relationships between the Kobs and (a) S_{BET}, (b) Fe content.

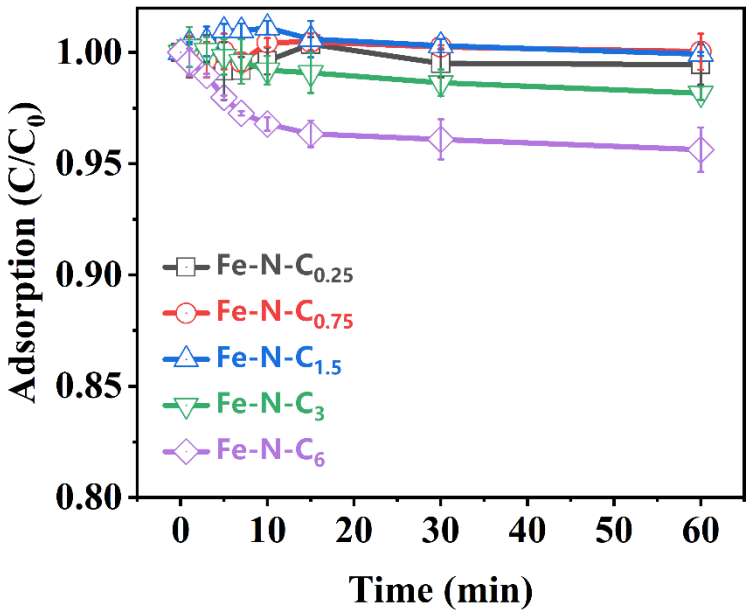


Figure S4. Adsorption performance of Fe-N-C_x. [catalyst] = 30 mg/L, [PCT] = 50 mg/L, pH_0= 5.8 (without pH adjustment), room temperature.

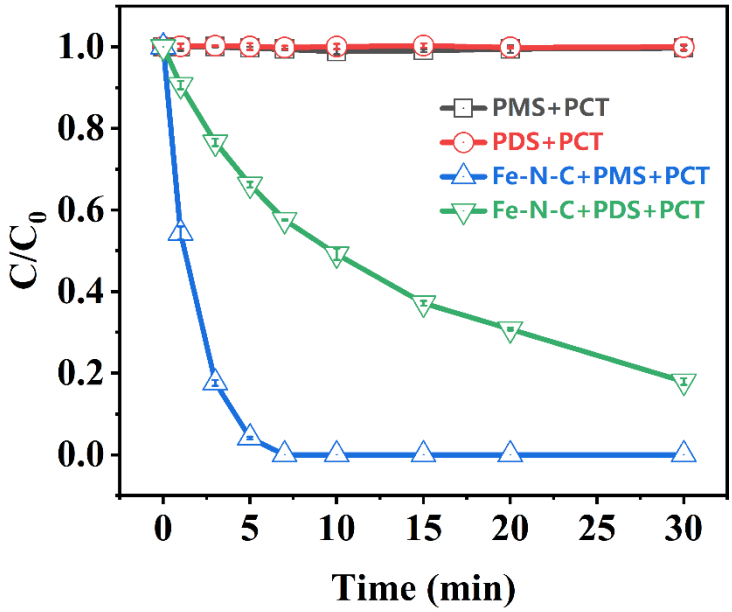


Figure S5. PCT degradation in different systems. [catalyst] = 20 mg/L, [PCT] = 10 mg/L, [PMS] = 1 mM, [PDS] = 1 mM, pH_0= 5.8 (without pH adjustment), room temperature.

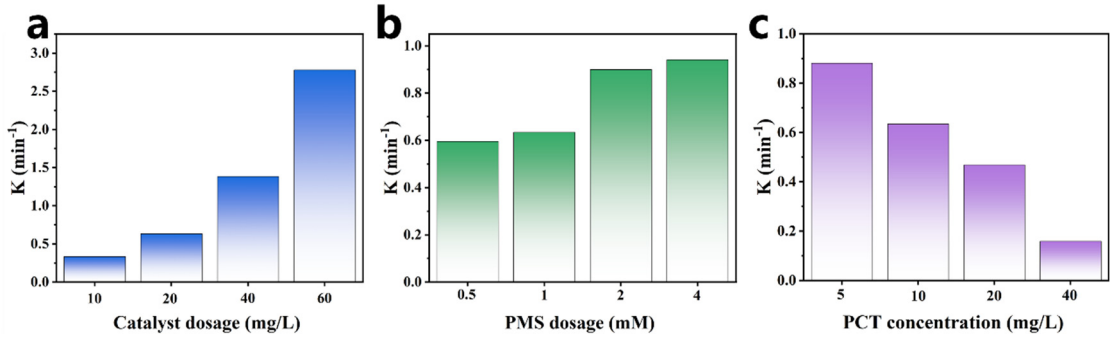


Figure S6. The first-order reaction rate constants of PCT degradation under different catalyst dosage (a), PMS dosage (b), PCT concentration (c).

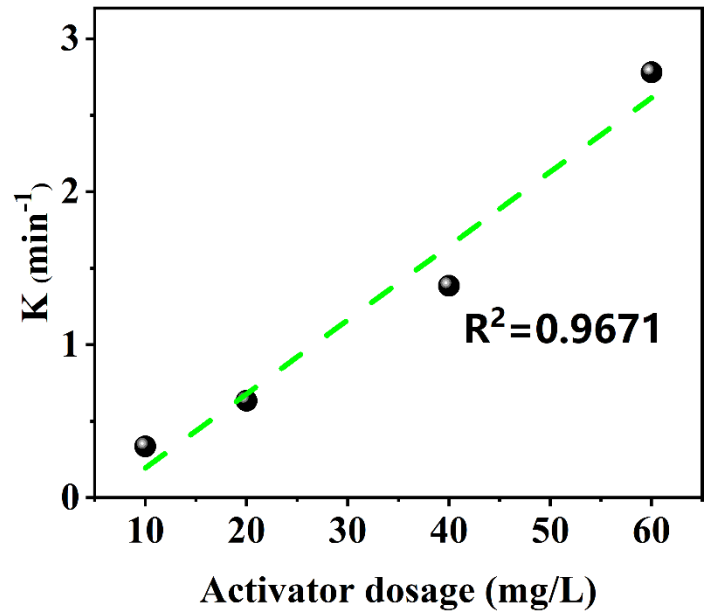


Figure S7. Catalyst dosages and linear fitting of first-order reaction rate constants.

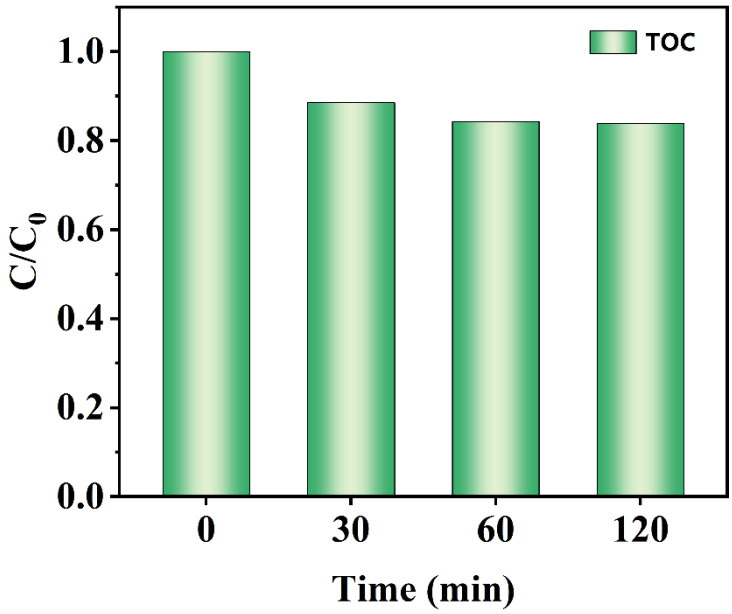


Figure S8. TOC removal of PCT degradation in the Fe-N-$C_{1.5}$/PMS system.

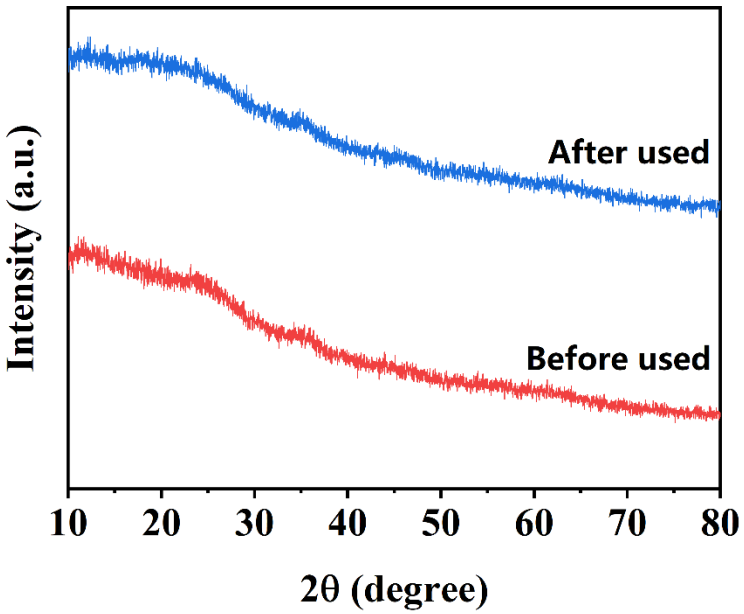


Figure S9. XRD patterns of Fe-N-$C_{1.5}$ before and after use.

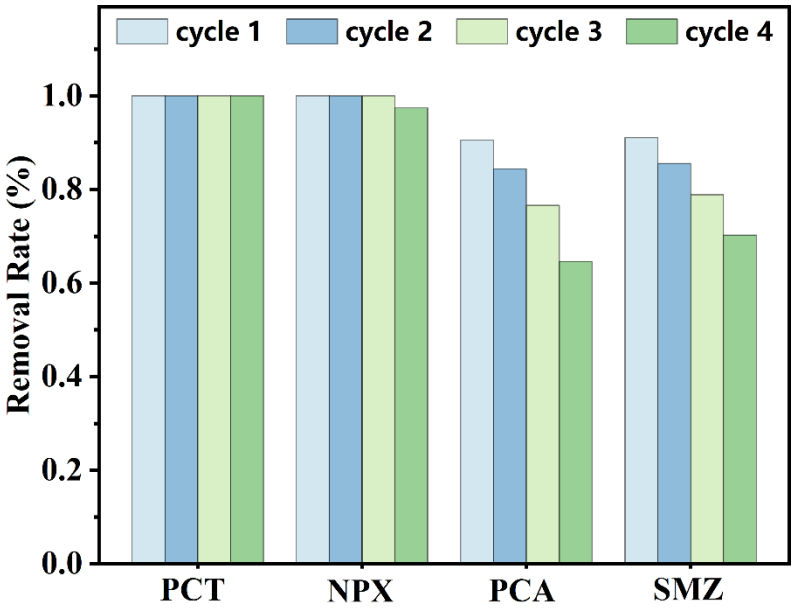


Figure S10. Cycle experiments for PCT, NPX, PCA, and SMZ. (reaction time per cycle: 180 min)

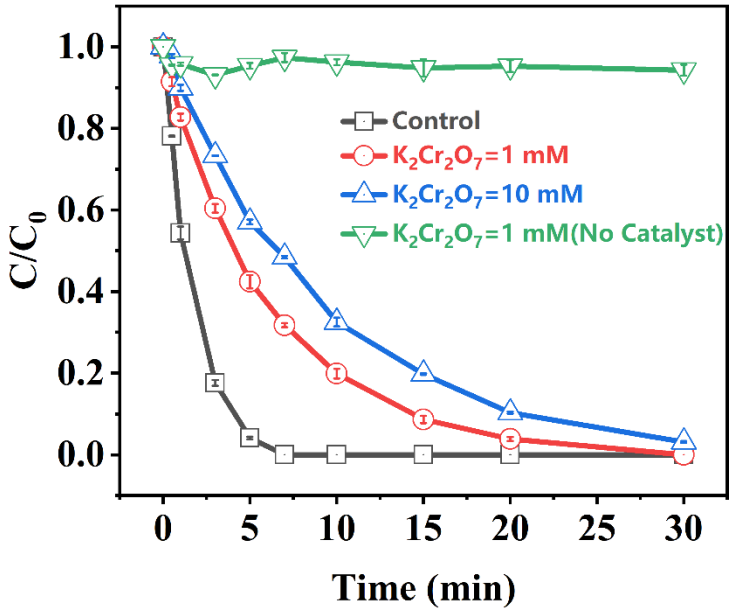


Figure S11. Effects of different concentrations of $K_2Cr_2O_7$ on Fe-N-$C_{1.5}$/PMS/PCT system. [catalyst] = 20 mg/L, [PCT] = 10 mg/L, [PMS] = 1 mM, pH_0= 5.8 (without pH adjustment), room temperature.

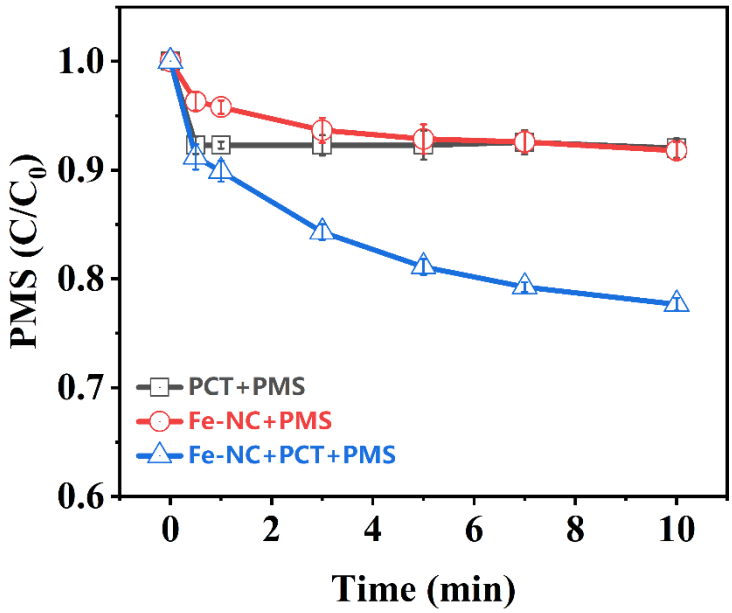


Figure S12. PMS decomposition in different systems. [catalyst] = 20 mg/L, [PCT] = 10 mg/L, [PMS] = 1 mM, pH_0= 5.8 (without pH

adjustment), room temperature.

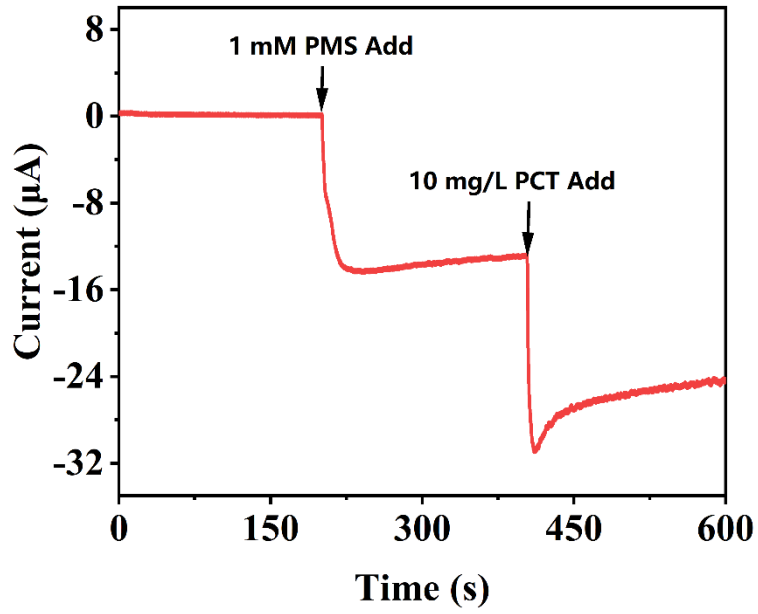


Figure S13. I-t experiment of Fe-N-$C_{1.5}$/PMS/PCT system.

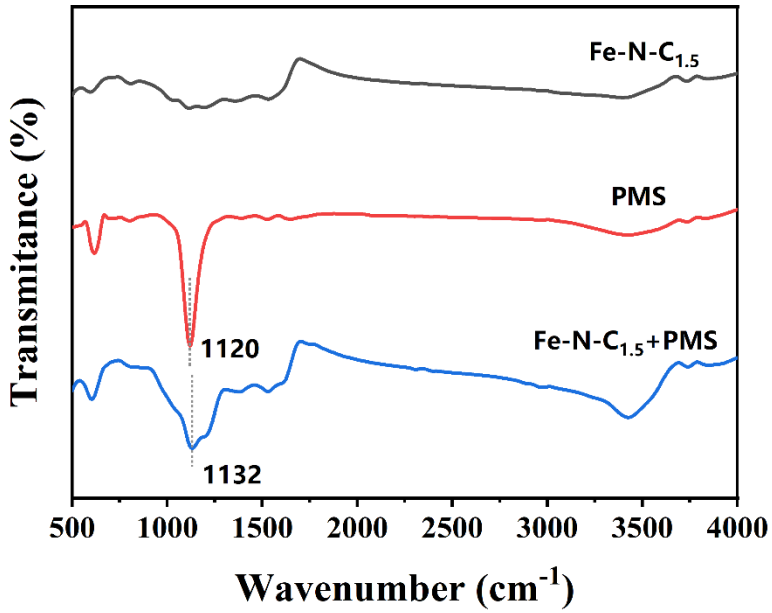


Figure S14. FTIR of Fe-N-$C_{1.5}$ only, PMS only and Fe-N-$C_{1.5}$/PMS.

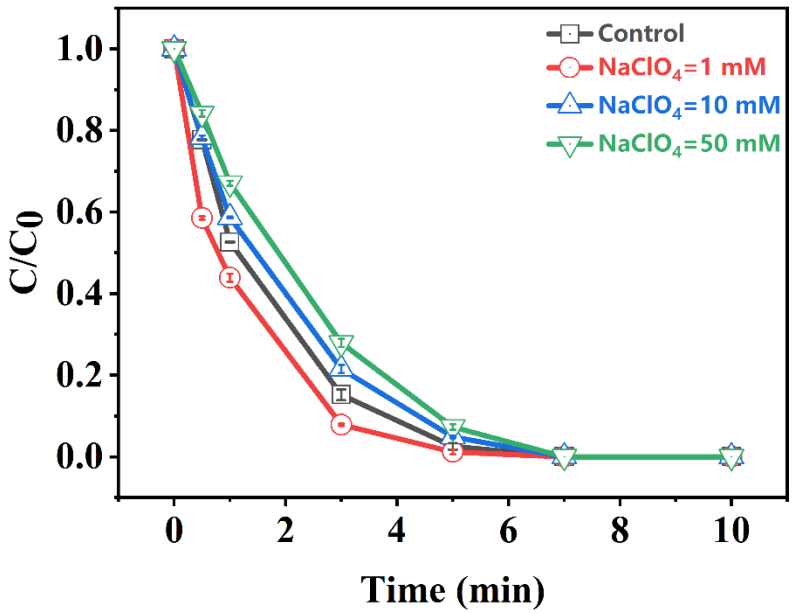
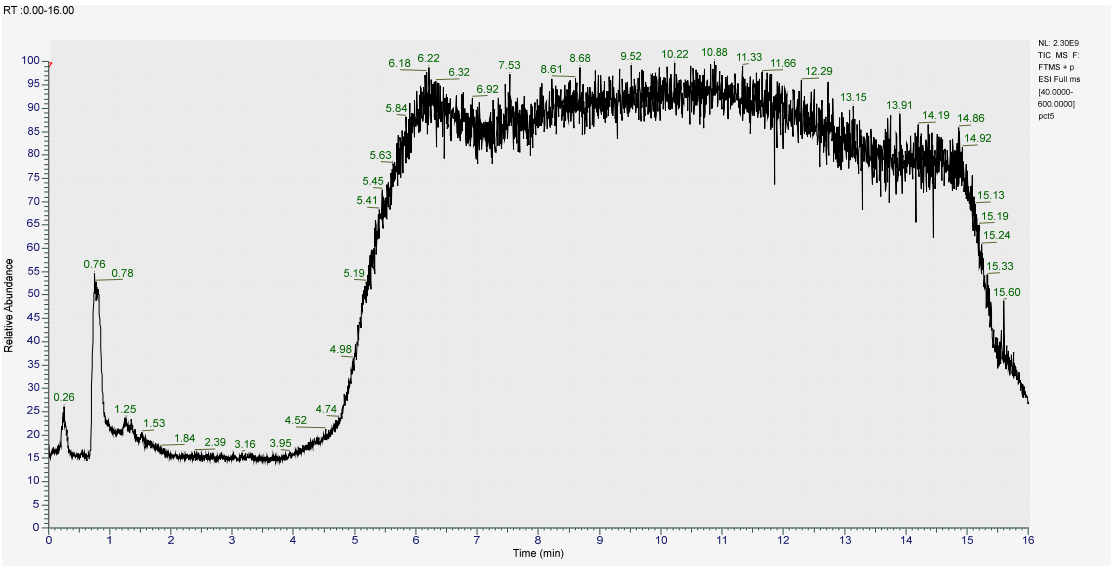


Figure S15. Effects of different concentrations of $NaClO_4$ on Fe-N-$C_{1.5}$/PMS/PCT system. [catalyst] = 20 mg/L, [PCT] = 10 mg/L, [PMS] = 1 mM, pH_0= 5.8 (without pH adjustment), room temperature.



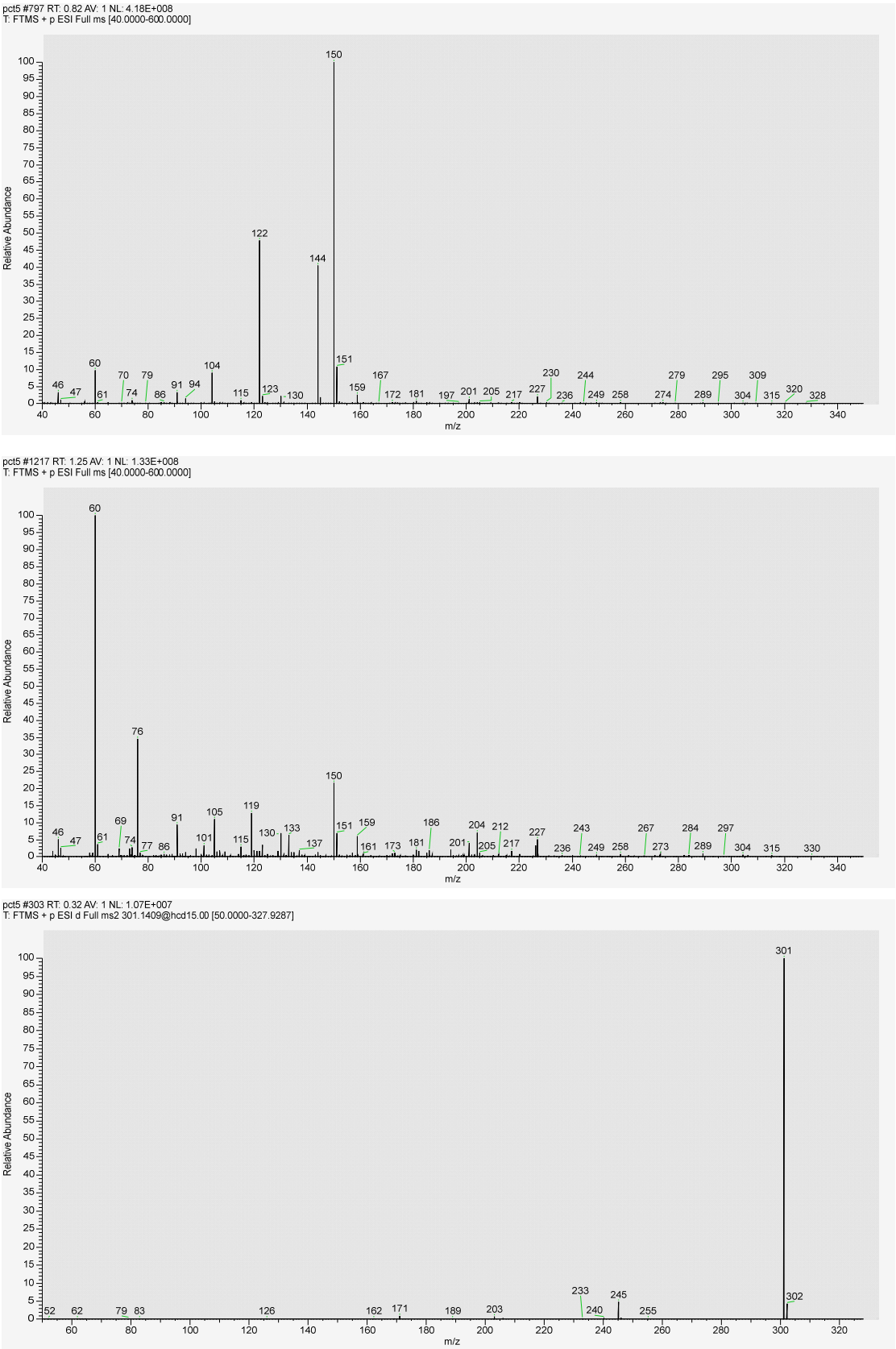


Figure S16. Chromatogram and mass spectrum of substances at 5 min.

References

1. Huang, K.Z.; Zhang, H. Direct Electron-Transfer-Based Peroxymonosulfate Activation by Iron-Doped Manganese Oxide (δ-MnO2) and the Development of Galvanic Oxidation Processes (GOPs). *Environmental Science & Technology* **2019**, *53*, 12610-12620, doi:10.1021/acs.est.9b03648.
2. Shi, J.; Dai, B.; Shen, X.; Xu, L.; Zhang, Y.; Gan, L. Wood induced preparation of Fe3C decorated biochar for peroxymonosulfate activation towards bisphenol a degradation with low ion leaching. *Journal of Environmental Management* **2023**, *340*, 117978, doi:https://doi.org/10.1016/j.jenvman.2023.117978.
3. Mohammadi, S.A.; Najafi, H.; Asasian-Kolur, N.; Ebrahimian Pirbazari, A.; Sharifian, S. The efficiency of a granular Fe-based metal-organic framework for the persulfate oxidative degradation of levofloxacin, an emerging antibiotic in wastewater. *Journal of Molecular Liquids* **2024**, *405*, 125119, doi:https://doi.org/10.1016/j.molliq.2024.125119.
4. Huang, M.; Wang, Y.; Wan, J.; Ma, Y.; Chi, H.; Xu, Y.; Qiu, S. Facile construction of highly reactive and stable defective iron-based metal organic frameworks for efficient degradation of Tetrabromobisphenol A via persulfate activation. *Environmental Pollution* **2020**, *256*, 113399, doi:https://doi.org/10.1016/j.envpol.2019.113399.
5. Zhu, K.; Bin, Q.; Shen, Y.; Huang, J.; He, D.; Chen, W. In-situ formed N-doped bamboo-like carbon nanotubes encapsulated with Fe nanoparticles supported by biochar as highly efficient catalyst for activation of persulfate (PS) toward degradation of organic pollutants. *Chemical Engineering Journal* **2020**, *402*, 126090, doi:https://doi.org/10.1016/j.cej.2020.126090.
6. Liu, J.; Zhu, J.; Zeng, X.; Yang, Y.; Zhang, G.; Sun, Y.; Fan, G. Enhanced activation of persulfate by bimetal and nitrogen co-doped biochar for efficient degradation of refractory organic contaminants: The role of the second metal. *Journal of Physics and Chemistry of Solids* **2024**, *193*, 112191, doi:https://doi.org/10.1016/j.jpcs.2024.112191.
7. Peng, L.; Duan, X.; Shang, Y.; Gao, B.; Xu, X. Engineered carbon supported single iron atom sites and iron clusters from Fe-rich Enteromorpha for Fenton-like reactions via nonradical pathways. *Applied Catalysis B: Environmental* **2021**, *287*, 119963, doi:https://doi.org/10.1016/j.apcatb.2021.119963.
8. Zhu, J.; Wang, L.; Hayat, W.; Zhang, Y.; Huang, S.; Zhang, X.; Zhou, S. The efficient degradation of paracetamol using covalent triazine framework-derived Fe-N-C activated peroxymonosulfate via a non-radical pathway: Analysis of high-valent iron oxide, singlet oxygen and electron transfer. *Separation and Purification Technology* **2023**, *310*, 123034, doi:https://doi.org/10.1016/j.seppur.2022.123034.
9. Li, X.; Chen, J.; Liu, Z.; He, C.; Pang, J.; Zhang, L.; Tang, F.; Yang, X. Recognizing the relevance of non-radical peroxymonosulfate activation by co-doped Fe metal-organic framework for the high-efficient degradation of acetaminophen: Role of singlet oxygen and the enhancement of redox cycle. *Chemical*

Engineering Journal **2024**, *499*, 156081, doi:https://doi.org/10.1016/j.cej.2024.156081.

10. Wang, T.; Liang, Q.; Xing, Y.; Sun, M.; Luo, H. Magnetic Fe/N-codoped carbon derived from modified Fe-base MOFs: Synergism of multiple active sites for peroxymonosulfate activation. *Journal of Environmental Chemical Engineering* **2023**, *11*, 109905, doi:https://doi.org/10.1016/j.jece.2023.109905.
11. Chen, C.; Ma, T.; Shang, Y.; Gao, B.; Jin, B.; Dan, H.; Li, Q.; Yue, Q.; Li, Y.; Wang, Y.; et al. In-situ pyrolysis of Enteromorpha as carbocatalyst for catalytic removal of organic contaminants: Considering the intrinsic N/Fe in Enteromorpha and non-radical reaction. *Applied Catalysis B: Environmental* **2019**, *250*, 382-395, doi:https://doi.org/10.1016/j.apcatb.2019.03.048.